SCERPA Simulation of Clocked Molecular Field-Coupling Nanocomputing

(Article begins on next page)

SCERPA Simulation of Clocked Molecular Field-Coupling Nanocomputing

Yuri Ardesi, *Student Member, IEEE,* Giovanna Turvani, Mariagrazia Graziano, and Gianluca Piccinini

***Abstract*—Among all the possible technologies proposed for post-CMOS computing, the molecular Field-Coupled Nanocomputing (FCN) is one of the most promising. The information propagation relies on electrostatic interactions among single molecules, overcoming the need for electron transport, significantly reducing energy dissipation. The expected working frequency is very high, and high throughput may be achieved by introducing an efficient pipeline of the information propagation. Pipeline could be realized by adding an external clock signal that controls the propagation of data and makes the transmission adiabatic. In this paper, we extend the Self-Consistent Electrostatic Potential Algorithm (SCERPA), previously introduced to analyze molecular circuits with a uniform clock field, to clocked molecular devices. The single-molecule is analyzed by ab initio calculations and modeled as an electronic device. Several clocked devices have been partitioned into clock zones and analyzed: the binary wire, the bus, the inverter, and the majority voter. The proposed modification of SCERPA enables linking the functional behavior of the clocked devices to molecular physics, becoming a possible tool for the eventual physical design verification of emerging FCN devices. The algorithm provides some first quantitative results that highlight the clocked propagation characteristics and provide significant feedback for the future implementation of molecular FCN circuits.**

***Index Terms*—Field-Coupled Nanocomputing (FCN), Molecular Quantum-dot Cellular Automata (MQCA), Algorithm, Multiphase clock.**

I. Introduction

FIeld-Coupled Nanocomputing (FCN) is one of the most promising technologies proposed for the post-CMOS scenario. Local field interaction among nanometric elements enables the propagation and the elaboration of the information with no charge transport, extremely reducing the power dissipation. Among the possible implementations [1]–[3], molecular FCN is one of the most attracting. The nanometric size of molecules enables digital computation at very high frequency, guaranteeing extremely high on-chip device density and possible room temperature operations [4], [5].

The molecular FCN relies on the Quantum-dot Cellular Automata (QCA) paradigm [6]. The basic element is the so-called QCA cell: a square-shaped cell composed of six quantum-dots with two mobile charges. The position of charges in the dots defines the logic information. In molecular FCN, redox centers favor the aggregation of the electron cloud in precise regions of the molecules, acting as charge aggregation points and playing the role of QCA dots. In this work, we consider the bisferrocene molecule, shown in Fig. 1(a), ad-hoc synthesized for realizing molecular FCN [7], [8]. This molecule is composed of three redox centers. Thus, two molecules are juxtaposed to create the molecular FCN cell, see Fig. 1(b). The position of charges in the molecular cell encodes the binary information, see Fig. 1(c).

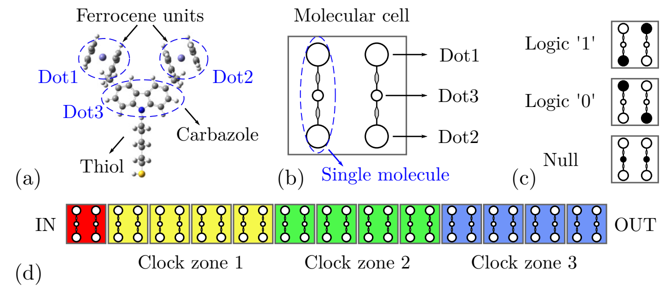

Fig. 1. (a) Molecular structure of the bisferrocene molecule. Logic (*Dot1*,*Dot2*) permits the information encoding; central (*Dot3*) alows the *Null* state encoding. (b) Schematic of a complete molecular FCN cell composed of two bisferrocene molecules (TOP VIEW). (c) Encoding of the information in molecular FCN cells. Two oxidation charges highlighted with black filled dots distribute along with the antipodal site of the cell, encoding the logic '0' or '1'. If charges occupy the central dots, the cell encodes the *Null* state. (d) Clocked molecular FCN wire partitioned with three clock zones represented by the three different colors.

By arranging cells in specific layouts, it is possible to build molecular wires and logic gates. The electrostatic repulsion enables the information to propagate. To avoid metastable conditions and guarantee correct information propagation, only a limited number of cells should be positioned side-by-side. Fig. 1(d) shows a clocked molecular wire. The circuit is partitioned into different clock zones, and a multi-phase clock system is applied [9]. An external signal, named clock field, facilitates the switching of cells in the clock zone [10], guaranteeing the so-called *Adiabatic Switching* [9], [11], [12]. The multi-phase clock also guides the information propagation in FCN circuits, eventually increasing the throughput thanks to an efficient pipeline system [4], [12].

The layout partitioning introduced by the clocking mechanism is an essential element of FCN design tools, which must allow the designer to compose the digital circuit layout by considering the clocking issue [13]. For instance, QCADesigner analyzes general clocked QCA devices with high-level quantum mechanical model [14]. Considering molecular FCN, there is a specific need for sophisticated tools [15], with computational capability, to evaluate the information propagation by maintaining a strong link with the physics at the

Y. Ardesi, G. Turvani, and G. Piccinini are with the Department of Electronics and Telecommunications, Politecnico di Torino, Torino, 10129, Italy. M. Graziano is with the Department of Applied Science and Technology, Politecnico di Torino, Torino, 10129, Italy.

Corresponding Author e-mail: yuri.ardesi@polito.it

Manuscript received March 8, 2020.

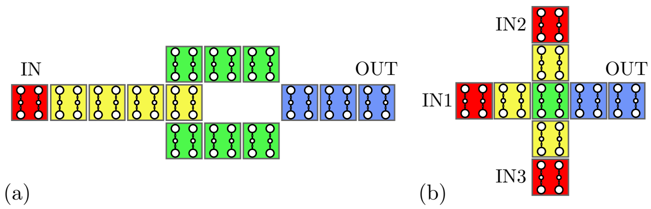

Fig. 2. (a) Clocked molecular FCN inverter partitioned into three clock zones represented by the three different colors. The information propagates from the first clock zone (yellow) to the two lateral branches (green). The inversion occurs at the interface between the two branches and the third clock zone (blue). (b) A three-input clocked molecular FCN majority voter: the logical output corresponds to the most recurrent logical input.

molecular scale. According to the authors' knowledge, unlike for example, in other emerging technologies [16], there is no available tool analyzing clocked molecular FCN considering the effective physics at the molecular scale.

Indeed, in [17], we proposed an iterative algorithm, named Self-Consistent ElectRostatic Potential Algorithm (SCERPA), to simulate molecular wires with uniform clock fields. The tool has been recently enhanced in [15] to permit the analysis of large circuits. Accurate ab initio calculations only characterize the single-molecule. SCERPA employs electrostatic equations to describe the intermolecular interaction, permitting physical simulation overcoming the use of full ab initio calculation for the whole circuit analysis. Ab initio calculation is suitable for computing molecular properties, yet extremely computationally expensive, making large circuit analysis unfeasible.

At the state-of-the-art, the algorithm has been used only to study the propagation in non-clocked devices [15], [18], [19]. In this work, we extend SCERPA to simulate clocked circuits. We partition different devices (the wire, the inverter, the majority voter, the bus, and the xor) into clock zones, and we analyze the information propagation. The enhanced algorithm evaluates the charge distribution of molecules, demonstrating the information propagation in clocked molecular circuits and highlighting novel results on the information propagation in the molecular FCN devices. The results show a mismatch between general QCA expectations and the obtained physical simulations, motivating our work to seek alternative tools providing a more robust link with molecular physics.

The clock influence is modeled with a physical perspective by considering the influence an electric field has on a molecule, assessed with ab initio calculation. Each molecule of the circuit could be subjected to a different clock field, giving SCERPA the flexibility to analyze molecular circuits considering the effective clock field imposed by the technological structure. SCERPA enables the physical-aware design of logic circuits and fulfills our aim to analyze the effects of clock fields on information propagation effectively. This tool provides feedback to technologists for realizing clock electrodes and favors the eventual realization of a working prototype with a feasible and reliable clocking topology.

II. Background

A. The molecular Field-Coupled Nanocomputing

Among the possible Field-Coupled Nanocomputing (FCN) implementations, the molecular FCN is one of the most promising: molecules are prone to ambient temperature operations, allow extremely high device density on the chip, and the expected operating frequency is very high [3], [20], [21].

Molecules can be oxidized (losing an electron) to increase the intermolecular electrostatic interaction and to facilitate the information encoding [22], [23]. Molecule redox centers allow the charge distribution (i.e. the electron cloud) to aggregate in precise points of the molecule. If two oxidized molecules are juxtaposed, Fig. 1(b), the positive charges repel each to the other. The charges occupy the two antipodal sides, creating the two possible states encoding logical states '0' and '1'. The information encoding in molecular FCN relies on the Quantum-dot Cellular Automata (QCA) concept: the single QCA cell is formed by six quantum-dots organized in a square-shaped configuration, as previously shown in Fig. 1(c). Moreover, in the six-dot QCA cell, a *Null* state can be encoded by forcing charges to occupy the central dots using an external electric field. The *Null* state does not encode any information, yet, it is necessary to guarantee the adiabatic switching [11].

The single-cell undergoes the electrostatic influence of neighbors, adapting its charge distribution and, consequently, the logical state. General-purpose computing is achieved by arranging cells [24]: molecular wires, logic gates, and even simple microprocessors were proposed within the general QCA paradigm [3], [24]–[26]. In particular, the wire consists of several cells arranged in a row, as previously shown in Fig. 1(d). Fig. 2(a) shows a possible inverter whereas Fig. 2(a) depicts a majority voter: a three-input logic device which outputs the most recurrent logical input (i.e. the output is '1' if at least two of the logical inputs are'1'). These logic structures are essential to design more complex digital circuits.

B. Fabrication of QCA technologies

The FCN paradigm has been demonstrated experimentally on several technologies, e.g. metallic [1] and magnetic [2]. Concerning the molecular FCN, resolution requirements are high, slowing down the experimental verification. Several molecules have been deposited, demonstrating the possibility to have self-assembled monolayers [8], [27]. Hydrogen depassivation lithography, nanoshaving, and Scanning Tunnelling Microscopy are promising for nanopatterning self-assembly monolayers [28], [29]. A second crucial point regards the realization of a write-in and a read-out system. Electrodes can be used to create an electric field polarizing molecules [20]. Single-electron transistors, eventually realized at the molecular scale, are instead promising to realize integrable charge sensors [30]. At the research level, Kelvin-Probe Microscopy is also interesting for imaging the charge of molecules [31].

C. The bisferrocene molecule

The bisferrocene molecule, considered as a reference in this work, has been synthesized ad-hoc for implementing molecular FCN [7], [8]. Fig. 1(a) reports the molecular structure of the *bisferrocene* molecule and highlights the redox centers (i.e. the charge aggregation points). The two ferrocenes act as logic dots (*Dot1* and *Dot2*); the central carbazole group, central dot *Dot3*, is used to encode the *Null* state. An alkyl-chain ended with a (-SH) component anchors the carbazole to the gold substrate [32]. The three bisferrocene redox centers play the role of QCA dots, see Fig. 1(b). It is possible to create a complete cell by juxtaposing two molecules.

Two mobile charges are introduced in the complete cell as holes (one charge per molecule) by electrochemistry techniques, to achieve optimum performance [10], [23]. A -1 e negative charge is fixed as a counterion to guarantee the neutrality of the molecule [27].

D. Clock zones and clock signals

As already mentioned in Section I, to avoid the generation of logic errors during the switching of cells, only a limited number of cells can be cascaded. Thus, complex FCN circuits are partitioned into small clock zones, and different clock signals are applied to each of them, guiding the switching of cells between *Null* and active states (Logic value '0' or '1').

Regarding the molecular FCN wire, shown in Fig. 1(d), the device is designed to ensure data flow through three adjacent clock zones and a well-designed multi-phase clock system [33]. Two electrodes generate the clock electric field (i.e. the clock signal) orthogonal to the information propagation direction, as depicted in Fig. 3(a).

When the clock field is downward-directed, the charge is trapped to the third dot, encoding the *Null* state, and disabling the information propagation. Conversely, an upward-directed clock field releases the charge from the third dot, consequently enhancing the interaction among molecules. The transition from the negative to the positive clock (and vice versa) advances gradually to ensure the quasi-adiabatic switching and to avoid metastable conditions [11]. In particular, four possible phases (i.e. four possible clock cell states), see Fig. 3(b), determines the role of each cell in the circuit:

- **Switch phase**: the positive molecular charge in the molecule is gradually pushed toward the two logic dots by applying an increasing ramp clock signal. Molecules can polarize under the influence of neighboring cells.
- **Hold phase**: charges are kept trapped in the active dots of the molecules by a fixed positive clock; the cell polarization is retained without further switching phenomena.
- **Release phase**: the positive molecular charge is gradually pushed toward the third dot by applying a decreasing ramp clock signal. The intermolecular interaction (i.e. the information propagation) is gradually disabled.
- **Reset phase**: charges are kept fixed in the third dot of molecules by a negative clock; all the molecules are maintained in the *Null* states and switching is not allowed.

The four phases together constitute the so-called *clock cycle*. Besides, the layout of circuits is partitioned into clock zones, Fig. 2, and four periodic clock cycles, shifted by a quantity $\pi/2$ (i.e. 1/4 of the signal period T), control the molecule of each clock zone to ensure the correctness of information propagation, as depicted by Fig. 3(c). The clock system also introduces a pipelining system which enables high throughput. Finally, the clock provides the true power gain necessary to maintain signal energy, which would otherwise decay due to inelastic losses [34].

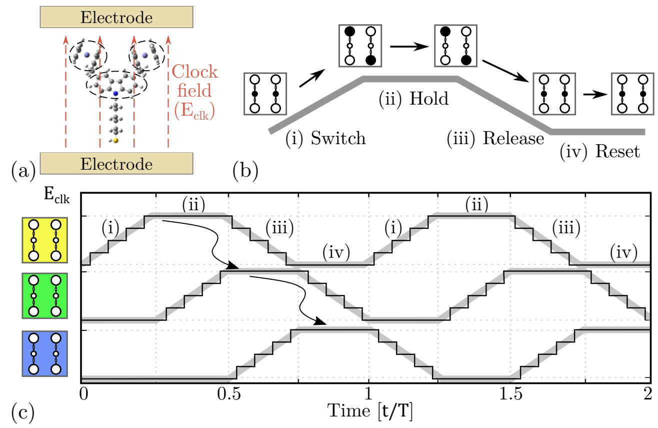

Fig. 3. (a) Generation of clock field through electrodes; the field is perpendicular to the active dots axis and can push the charge in the active dots or the central dot according to electric field direction; (b) Detailed representation of a single clock cycle used in molecular FCN technology with its four phases. (c) Periodic application of the clock cycles on the three clock zones; the arrows demonstrate the flow of information from a zone to the adjacent one. SCERPA approximates the clock signals with trapezoidal staircase functions.

E. Simulation of molecular FCN devices

Ab initio calculation can be used to analyze single molecules or molecular cells (2 molecules together), yet the considerable computation cost and the necessity of time-varying clock signals obstruct the possibility to simulate complex but fundamental molecular logic devices [17]. An alternative method was proposed in [35]: it analyses a molecular wire by performing several ab initio calculations. In this case, the ab initio computation analyses one molecule at-a-time. Indeed, following the wire propagation direction, each molecule was studied by emulating the prior molecule with point charges. In a more realistic case, all the molecules in the circuit interact with each other. For these reasons, we proposed a new algorithm in [17], which models the molecule with the so-called MosQuiTo (Molecular Simulator Quantum-dot cellular automata Torino) methodology and evaluates the interaction with electrostatic equations, overcoming the need of ab initio calculation for evaluating the information propagation. The algorithm, named Self-Consistent ElectRostatic Potential Algorithm (SCERPA), has been recently optimized in [15], to simulate large circuits efficiently, considering the effective behavior of molecules.

F. The Self-Consistent Electrostatic Potential Algorithm

SCERPA evaluates, using an iterative procedure, the voltage generated by each molecule, and the consequent molecular charge distribution, exploiting the transharacteristics [23]. The absence of DFT calculation in the evaluation procedure makes the algorithm very fast, enabling the evaluation of hundreds of molecules in a few seconds [15]. The single-core DFT calculation of the bis-ferrocene charge distribution requires more than an hour. A wire composed of ten molecules under a uniform clock field requires 175 SCERPA steps (damping 0.4), evaluated in less than a second. By assuming an optimistic DFT complexity $O(N)$, with N denoting the number of atoms, DFT would require more than two months. Notice that real DFT complexity reaches $O(N^4)$ when using hybrid functionals [36]. SCERPA considers the molecule electrostatic potential, evaluated with the aggregated charge model, always to mimic the isolated molecule. This assumption reduces the SCERPA computation cost, even though prevent SCERPA from considering possible alterations caused by hindrance effects and introduces a small error in the evaluation of the intermolecular interaction. We demonstrated in [15], [23] that the estimated error for average intermolecular distance is small and surely acceptable if one considers that a complete ab initio calculation is not feasible. Indeed, distinct molecules are not supposed to compenetrate orbitals in molecular FCN. The aggregated charge model permits an accurate evaluation of the molecular electrostatic potential.

At the state-of-the-art, SCERPA has been used to study molecular wires, eventually taking into account substrate defects [18]. In this work, we extend SCERPA to simulate clocked molecular FCN devices. The algorithm is currently implemented as a MATLAB code, deeply discussed in [15]. The tool requires the definition of a molecular layout, declaring each molecule's position. SCERPA evaluates the ground-state configuration of molecules in a discretized set of timesteps. The molecular charge of some molecules can be defined by the user to create "drivers". The evaluation never modifies driver charges. SCERPA requires a driver table defining the value of driver molecules at each timestep. Similarly, a clock table details the molecule clock fields at each timestep. These two tables permit examining pipelined clocked molecular circuits, favoring the circuit-level study of clocked molecular devices, proceeding towards assessing molecular FCN as a possible candidate for the beyond-CMOS scenario.

III. METHODOLOGY

Many articles [3], [22], [23], [32], [37] deeply analyze the intermolecular interaction to validate the molecule as a candidate to realize FCN computation.

In this paper, we want to evaluate the information propagation in clocked molecular circuits considering the effects of the clock system. The methodology is subdivided into four parts: molecule characterization, counterion introduction, multi-phase clock assignment, and algorithm implementation.

Notice that this work analyses circuits constituted by the bis-ferrocene molecule, which is used as a reference. The method and the tool are general and can be applied to any molecule provided its description, as demonstrated in [15].

A. Molecule characterisation

The bis-ferrocene molecule is modeled and studied following the so-called MoSquiTo methodology [23], [37]. To derive the essential properties of the molecular interaction, we employ the DFT by using *Gaussian 09* [38]. *UB3LYP* and *LANL2DZ* are chosen as suitable functional and basis set respectively [10], [23].

In particular, as sketched in Fig. 4(a), two bisferrocene molecules, considered as *Driver* and *Molecule-Under-Test (MUT)*, are juxtaposed. The bis-ferrocene has three aggregated charges, thus both Driver and MUT are modelled by three point charges. *Driver* charges *D1*, *D2* and *D3*, representing the two logic dots and the central dot of a bisferrocene molecule, generate an electric field that can be "measured" between the positions of the *MUT Dot1* and *Dot2*, this value is named MUT input voltage $V_{in,MUT}$. The *MUT* re-arranges the distribution of the aggregated dot charges *Q1*, *Q2* and *Q3* on the three dots, see Fig. 4(b). The correlation between the aggregated charges and the input voltage defines the Vin-Aggregated Charge Transcharacteristics (VACT). It permits the evaluation of the intermolecular interaction independently on the position of driver and MUT in the circuit, indeed, the same procedure can be applied to *MUT'* in Fig. 4(b). The transcharacteristics also depend on the clock field value, thus, dealing with clocked devices, the same procedure is repeated to obtain the VACT with different values of the clock field E_{clk}. Finally, the different aggregated charges are linked to the corresponding input voltage V_{in} and clock field E_{clk} to obtain the clock dependent VACT. The generic aggregated charge of a dot (Q_α) can be expressed as:

$$Q_{\alpha,i} = Q_\alpha(V_{in,i}, E_{clk,i}) \tag{1}$$

Where V_{in} is the input voltage of the generic *Molecule i*.

B. Counterion introduction

As mentioned in Sec. II, the single-molecule is coupled with a -1 e negative charge (counterion) to guarantee the neutrality of the molecule [27]. In 2D circuits, the presence of the counterion is significant. Indeed, the non-neutrality of the wires creates a crosstalk effect, which impinges on the information propagation. Fig. 4(d) shows the effect of not considering the counterion on two parallel molecular wires. To limit the crosstalk, *Dot3* aggregated charge is reduced by a quantity -1 e to model the introduction of the counterion.

$$\bar{Q}_3 = Q_3 - 1e \tag{2}$$

Q_3 is the physical aggregated charge of *Dot3*, obtained from ab initio calculation, whereas $\bar{Q}_3$ is the charge used in the algorithm to consider the counterion. This modification shields the molecule by making it neutral, and improves the robustness of the information propagation, see Fig. 4(e).

1) Multi-phase clock assignment: Differently to the previous version of SCERPA [15], which mainly consider non-clocked wires to demonstrate the working principle of the algorithm and analyze the computational cost, we here consider 1D-2D clocked circuits. The layout of the molecular circuit is partitioned into clock zones to guarantee the information propagation correctness. Each clock zone has a clock signal that activates cells and controls the information flow.

To be specific, Fig. 4(c) depicts the schematic implementation of the physical clock system for a molecular wire. Three

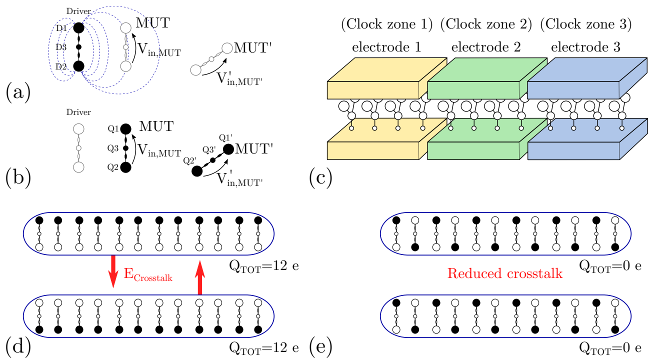

Fig. 4. (a) Driver molecule modelled by the three point-charges *D1*, *D2*, and *D3* emulating its logic and central dots. The driver generates an electric field which influences the *Molecule-Under-Test (MUT)*. The input voltage V_{in}, which depends on the position of the MUT, measures the driver influence. (b)The MUT aggregated charges re-arrange according to the input voltage V_{in}. (c) Schematic implementation of the clock electrode system of a molecular FCN wire partitioned into three clock zones. (d) Two parallel molecular wires: the counterion is not considered. The total charge of each wire, 12 e, generates an electric field that induces the polarisation of the other wire molecules (crosstalk). (e) Two parallel molecular wires: the counterion is considered. The total wire charge is null. The crosstalk strongly reduces.

pairs of electrodes define the clock zones by embracing groups of four molecules; the time-varying electric field is applied through the system of electrodes. As discussed in Section II, Fig. 3(c) highlights the periodic four-phase clock signal generated by applying a voltage to each pair of electrodes associated with the three clock zones of Fig. 4(c). For simplicity, we consider the electric field of the clock signal equal for all the molecules in the same clock zone. In this work, we do not address the problem of switching speed. Indeed, slowly-varying trapezoidal signals model the time evolution of the clock field. We assume the molecules switch slowly enough to guarantee the quasi-adiabatic switching, i.e. they always lie in their ground state configuration, minimizing the energy consumption [39].

C. Algorithm implementation

The working principle of SCERPA, which is implemented in MATLAB, is deeply discussed in [15]. It consists of four main stages (initialization, selection, interaction, and output) that we here modify to consider the clock field independent for each molecule. Algorithm 1 reports the pseudocode of SCERPA, considering the modifications made in this work.

1) Initialization stage: SCERPA starts by importing the layout of the circuit composed of N molecules, currently generated with a MATLAB script. Some molecules are marked as drivers so that their driver charge distribution will be considered fixed by the evaluation procedure. Dealing with time-varying signals, the time is discretized on a number T of time steps $\{t_0, \cdots, t_T\}$. SCERPA initially creates an $N \times T$ matrix, denoted as clock field table. The element $\{i, \tau\}$ is the clock field $E^{\tau}_{clk,i}$ associated to *Molecule i* at the instant t_τ. The polarisation of driver molecules is also time-varying; thus V^{τ}_D denotes the input voltage generated by all driver molecules on a generic *Molecule i* at time t_τ. The input script providing the circuit layout also provides the clock field and driver tables.

Algorithm 1 Pseudocode of the proposed algorithm.

```
Initialization of molecular Layout;                         ▷ Initialization stage
Initialization clock field and driver tables;
for each molecule as i do
    for each molecule as j do
        if distance (i,j) < d_IR then
            Insert j in the IR list of i;
for each Step τ do                                          ▷ Selection stage
    Evaluate driver effects V_D^τ;
    UpdateDriverEffects();
    UpdateClockEffects();
    while |dV| < ε_max do                                   ▷ Evaluation stage
        ComposeARList();
        for each molecule in AR list as i do
            V_in,i = V_D,i;
            for each molecule in IR list of i as j do
                V_i,j = EvaluateMoleculeContribution(i,j);
                V_in,i = V_in,i + V_j,i
        Evaluate the Voltage Variation (dV_i)
Output the final charge distribution                        ▷ Output stage
```

Also, SCERPA evaluates in this stage the distance among all the circuit molecules. For each molecule, the procedure inserts all the neighbors within a specified radius in the so-called molecule Interaction Radius (IR) list.

2) Selection stage: As reported in [15], the input voltage of *Molecule i* ($V^{\tau}_{in,i}$) is evaluated by solving, at each time step (t_τ), the non-linear system:

$$V^{\tau}_{in,i} = V^{\tau}_{D,i} + \sum_{j \in IR} V^{\tau}_{j,i}(V^{\tau}_{in,j}, E^{\tau}_{clk,j}) \tag{3}$$

Where $V_{j,i}$ is the voltage generate by Molecule j on Molecule i, evaluated in the Interaction Stage. From a computational standpoint, equation 3 is solved iteratively as:

$$V^{k,\tau}_{in,i} = F_i(V^{k-1,\tau}_{in,1}, \cdots, V^{k-1,\tau}_{in,i-1}, V^{k-1,\tau}_{in,i+1}, \cdots, V^{k-1,\tau}_{in,N}) \tag{4}$$

Where k is the single-step of the iterative procedure and F_i denotes the equation (3). The iterative procedure is performed in each time step (t_τ). The initial guess at a generic time $V^{0,\tau}_{in}$ considers the state of the circuit at the previous time step, and the time-dependency of driver molecules. Indeed, the initial guess $V^{0,\tau}_{in}$ is set equal to the solution ($k = \infty$) of equation 4 at the previous time ($\tau - 1$), denoted $V^{\infty,\tau-1}_{in}$. To consider a possible driver driver variation, function *UpdateDriverEffects* removes the driver effect of the previous time ($V^{\tau-1}_D$) and insert the driver effect of the current timestep V^{τ}_D. From a practical point of view the initial guess $V^{0,\tau}_{in}$ is obtained as:

$$V^{0,\tau}_{in} = V^{\infty,\tau-1}_{in} - V^{\tau-1}_D + V^{\tau}_D \tag{5}$$

In addition to this, at every time step, the clock fields can vary. The trapezoidal clock cycles are implemented in the algorithm with staircase functions, as sketched in Fig. 3(c). The function *UpdateClockEffects* updates the value of the clock field of each molecule. We assume each segment of the staircase signal to be long enough to satisfy the adiabatic switching; for this reason, the clock field is considered constant in each timestep.

3) Evaluation stage: The input voltage of the generic *Molecule i* formally depends on the status (i.e. the input voltage) of all the other molecules, which, in turn, depends on the status of *Molecule i*. For this reason, an iterative procedure is necessary to correctly evaluate the charge distribution of all the molecules in the circuit.

The generic *Molecule i* is modelled by a set of three aggregated charges $\{Q_1^i, \cdots, Q_3^i\}$, in positions in $\{\boldsymbol{r}_1^i, \cdots, \boldsymbol{r}_3^i\}$. The function *EvaluateMoleculeContribution* the evaluate the effect any *Molecule i* (with input voltage obtained from equation 5) produces on neighbour *Molecule j* ($V_{j,i}$) by calculating the field generated by the aggregated charge. All molecule contributions ($V_{j,i}$) are summed to the driver contribution $V_{D,i}$.

The *Molecule i* is subjected to a precise clock field $E_{clk,i}$ that, together with the input voltage $V_{in,j}$, permits evaluating the aggregated charge Q_α^j through the transcharacteristics, reported in equation (1).

Thanks to the strong distance-dependence of the electrostatic interaction, we demonstrated in [15], that only a few - active - molecules effectively interact with neighbors in a generic step of the iterative procedure. In each time step (t_τ), SCERPA extracts the set of active molecules to define the Active Region (AR) list (ComposeARList function). In each time step, SCERPA evaluates the input voltage of the active molecules only, considering the effects of the molecules in the Interaction Radius (IR) list. In particular, molecules inserted in the AR list are the ones whose input voltage between consecutive steps (voltage variation dV) varies more than a predefined threshold (V_{AR}). By introducing the clock, SCERPA inserts all the molecule whose clock field $E_{clk,i}$ varies between consecutive time steps, and all the corresponding neighbors, in the AR list. This method allows SCERPA to consider possible variations in the molecule polarisation induced by the clock.

4) Output stage: When all timesteps are examined, SCERPA provides the charge distribution of the molecular circuit in each timestep. The results allow verifying the information propagation in the circuit by considering the effective electrostatic behavior of molecules and clock system.

IV. Results

The generality of SCERPA allows the tool to analyze any molecule, provided the transcharacteristics. In this section, we use the bis-ferrocene molecule as a reference to demonstrate the functionality of the tool to provide, for the first time, physical insights on clocked devices. The obtained results are based on physical simulation and allow the designer to design digital devices considering possible molecular physics implications. First, we derive the response of the molecule to the clock field. Then, we study possible applications of the proposed algorithm on some multi-phase structures: the wire, the bus, the majority voter, and the inverter. All the devices are partitioned into clock-zones and analyzed as possible examples. Uniform clock fields are applied to each clock-zone to implement a pipeline mechanism that allows the logical input to change while propagating the information. Finally, we analyze an XOR to demonstrate the functionality of SCERPA on a more sophisticated device and clocking layout.

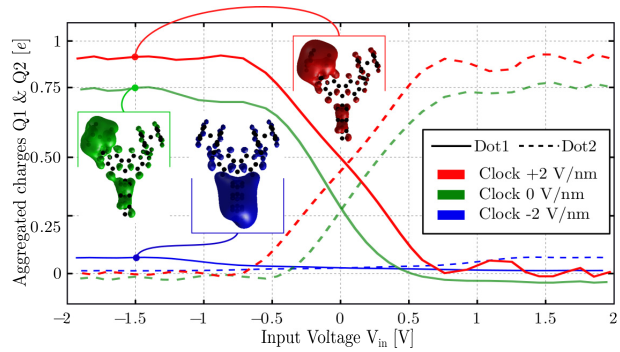

Fig. 5. Clock dependent Vin-Aggregated Charge Characteristics (VACT) of the bis-ferrocene molecule. 3D plots depict the molecule equipotential surfaces (potential is 3 V at the surface) in precise points of the transcharacteristics. According to the value of the input voltage V_{in}, with clock field is +2 V/nm, the charge fills *Dot1* or *Dot2*. If the clock is reduced to -2 V/nm, the charge is trapped in *Dot3* (hidden from the plot for the sake of clarity), strongly reducing the charge in the logic dots.

A. Clocked bis-ferrocene molecule

As mentioned in Section II.D, the clock-dependent transcharacteristics describe the molecule-to-molecule response for different clock fields. Fig. 5 shows the aggregated charges of logic dots (*Dot1* and *Dot2*) evaluated for three significant values of the clock field. The plot also shows the molecular equipotential surfaces evaluated by fixing the potential generated by the molecule to 3 V.

When the clock field is +2 V/nm, the charge fills one of the two logic dots, depending on the driver polarization. Considering a negative V_{in}, the charge mainly locates on *Dot1*. Charge on *Dot1* is almost null. The charge distribution scratches the equipotential surface, which enlarges around the *Dot1* ferrocene. With the -2 V/nm clock field, the charge on logic dots becomes negligible. In this case, the charge locates on *Dot3*, and the equipotential surface enlarges on the thiol.

When clock field is null, the aggregated charges on *Dot1* and *Dot2* decreases. With respect to the positive clock field case, the aggregated charge trapped in *Dot3* slightly increases.

B. The molecular wire

Molecular wires are deeply analyzed in [15] without considering clock phases. In this work, a molecular wire made up of 24 bis-ferrocene molecules is partitioned into three clock zones made by eight molecules each. The clock field is applied with the signals indicated in Fig. 3(c). Two complete clock cycles enable propagating both '0' and '1' logical values in a pipeline mechanism. Fig. 6 shows the electric potential distribution generated by the aggregated charge of the molecular wire during the propagation of the information.

At $t = 0$, all the molecules of the wire are in the *Reset* phase, and each molecule charge mainly locates on the low-localized central dots, generating a negligible field. As an example, for the first molecule after the driver, the

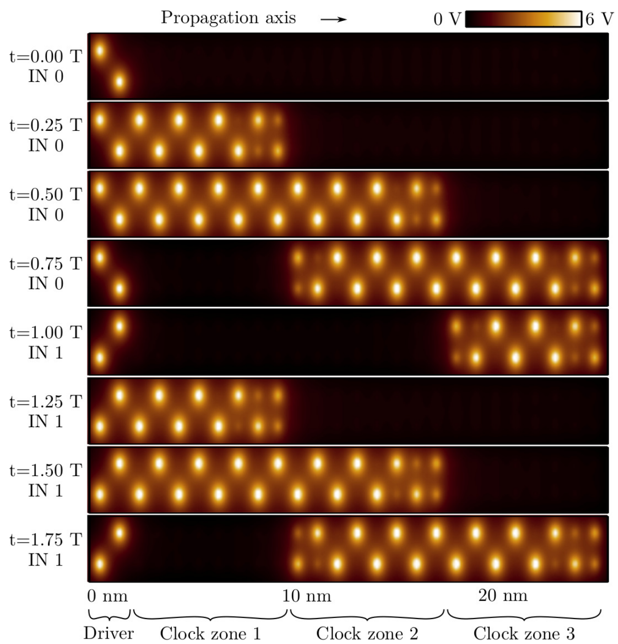

Fig. 6. SCERPA simulation of a clocked molecular FCN wire partitioned into three clock zones. Both logical values '0' and '1' are propagated in a pipeline mechanism. The figure reports the electrostatic potential generated by molecule charge distribution evaluated 0.2 nm above the active dot plane.

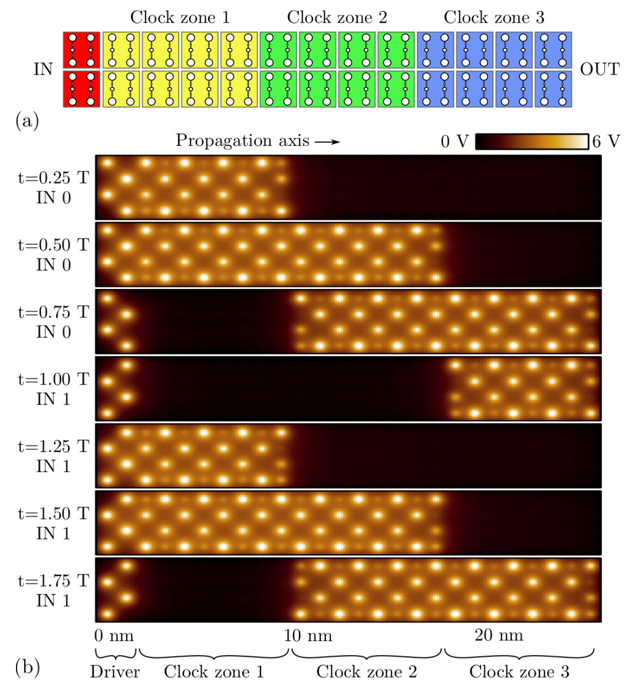

Fig. 7. (a) Layout of a clocked 2-lines molecular FCN bus partitioned into three clock zones. (b) SCERPA simulation of the clocked 2-lines molecular FCN bus. Two complete clock cycles are applied to propagate both '0' and '1' logical values in a pipeline mechanism. The figure reports the electrostatic potential generated by molecule charge distribution evaluated 0.2 nm above the active dot plane.

aggregated charges of logic dots are Q_1=0.023 e, Q_2=0.032 e, and $\bar{Q}_3$=-0.053 e (Q_3=0.947 e, without considering the counterion, see Sec. III-B). The charge separation between logic dots is not large enough to encode the information. The following molecules similarly follow: the interaction with other molecules is hardly noticeable.

At this point, SCERPA applies the increasing staircase trapezoidal function modeling the *Switch* phase to the first clock zone. For each step of the function, the algorithm solves equation 3 with the method described in Sec. III.

At $t = 0.25T$, the molecules of the first clock zone complete the *Switch* phase and enter the *Hold* phase. Consequently, with the input cell encoding '0', the aggregated charges of the first molecule after the driver are Q_1=0.010 e, Q_2=0.914 e and $\bar{Q}_3$=-0.925 e. For the following molecule Q_1=0.905 e, Q_2=0.010 e and $\bar{Q}_3$=-0.927 e. These two molecules have opposite polarization (i.e. *Dot2* charge is maximized in the first molecule, *Dot2* is minimized in the second one, also demonstrated by the potential distribution in Fig. 6) and define a cell encoding the same logical value of the input cell. All the cells in the first clock zone copy the input cell logical value, correctly propagating the information. Weaker charge separation in the last molecule of the first clock zone can be appreciated in Fig. 6); this is a typical border effect of molecular FCN technology [15], [19]. The cells of other clock regions are in the *Reset* phase, thus not active and not encoding information. By activating the second phase ($t = 0.5T$), the border effect disappears in the first phase, and it becomes appreciable at the end of the second phase. Moreover, at $t = 0.75T$, the second clock zone enters the *Release* phase.

At $t = T$, the second clock zone ends the *Release* phase and enters the *Reset* phase. The third clock zone enters the *Hold* phase. The information correctly propagates to the end of the wire, and the input cell is changed to encode the logic '1'. SCERPA updates the input voltage of all the molecules following equation 5. Notice that the driver is far from the third clock region and does not impinge on propagating the previous information. Finally, the same clock signals applied to clock zones in the period $[0, T]$ are replicated, correctly propagating the new information.

C. The 2-line molecular bus

Fig. 7(a) shows the layout of a clocked 2-line molecular FCN bus, where 2-lines means two adjacent molecular wires constitute the device. Fig. 7(b) shows the information propagation resulting from the SCERPA simulation. Comparing this result with the molecular wire, it is worth highlighting how a large number of molecules (i.e. molecular interactions) reduce the border effect, which is now hardly noticeable. The information is well-defined on the entire bus, which correctly propagates both the logical values '1' and '0'. Nevertheless, the 2-line bus exhibits a *skin effect*: a cross-talk between the two lines produces a bias in the voltage of all the molecules pushing the charge on the bus "skin". This effect does not impact the final propagation of the information; on the contrary, the 2-lines configuration correctly propagates both the logical values '1' and '0'. Multi-line devices are known in the general QCA paradigm as a countermeasure to technological defects such as missing cells [40]. In this work, we also highlight the resulting improvement of the encoding bistability. This evidence is novel and could not be noticed with a high-level simulator since it is linked with molecular physics. This result shows the advantage of using a simulator strongly linked with molecule physics and confirms the motivation to study clocked molecular devices with the SCERPA simulator. This result also provides essential feedback for the eventual fabrication of a molecular prototype. Indeed, the bus relaxes the constraints on the very high resolution required to manufacture molecular devices and optimizes the interaction among molecules, thus improving the information propagation.

D. The molecular majority voter

In a majority voter, the expected output corresponds to the most recurrent logical input (e.g. with inputs “0-1-0” the output is ‘0’). Fig. 8(a) shows the simulation of a clocked molecular majority voter obtained with SCERPA. Two logical ‘0’s and one logical ‘1’ are firstly assigned to the inputs, expecting output ‘0’. Then, at time $t = T$, the configuration of the inputs is changed by assigning three logical ‘1’s and expecting the majority voter to output ‘1’. The information propagates in the circuit guided by the clock signals.

At $t = 0.25T$, the first clock zone (CKZ1) is in the *Hold* phase and the associated molecules copy the logical value of the drivers. At the same time, the molecules of the central cell enter the *Switch* phase. At $t = 0.5T$, the first and the second clock zones (CKZ1 and CKZ2) are active and, most importantly, molecules located in CKZ2 (evaluation point) encode the logical value ‘0’, which is the expected logical output of the majority voter. The evaluation cell is inserted in a specific clock zone (CKZ2) to prevent the device from evaluating the majority function before logical inputs are stable. This layout emerges mandatory when the inputs have different delays (e.g. a different number of molecules forms the three input wires of CKZ1), Fig. 8(b). Finally, the device propagates the binary information towards the output cell (CKZ3), time $t = 0.75T$, Fig. 8(a). At $t = T$, the input configuration changes to “1-1-1”, and the device correctly outputs logical value ‘1’ after applying a second clock cycle.

For the first time, we demonstrate with physical simulations the possibility to create computation with molecules, confirming and refining the logic results examined so far in the literature with high-level quantum mechanical models.

For the sake of completeness, we also analyze a 2-lines molecular majority voter. Fig. 8(c) shows the obtained propagation after the application of a clock cycle (at $t = 0.75T$) with inputs “0-0-0” and “0-1-1”. In both cases, the output is consistent with expectations, demonstrating that the majority voter can also be created in a larger 2-line configuration.

E. The molecular inverter

Fig. 2(a) previously shown a possible molecular FCN inverter partitioned into three clock zones inherited from the general QCA paradigm. Fig. 9(a) shows the SCERPA simulation. All three clock zones are activated sequentially. It is straightforward to notice that the logical output can hardly be read, which means the inverter is not reliable when made with the bis-ferrocene molecule. This result highlights the need for

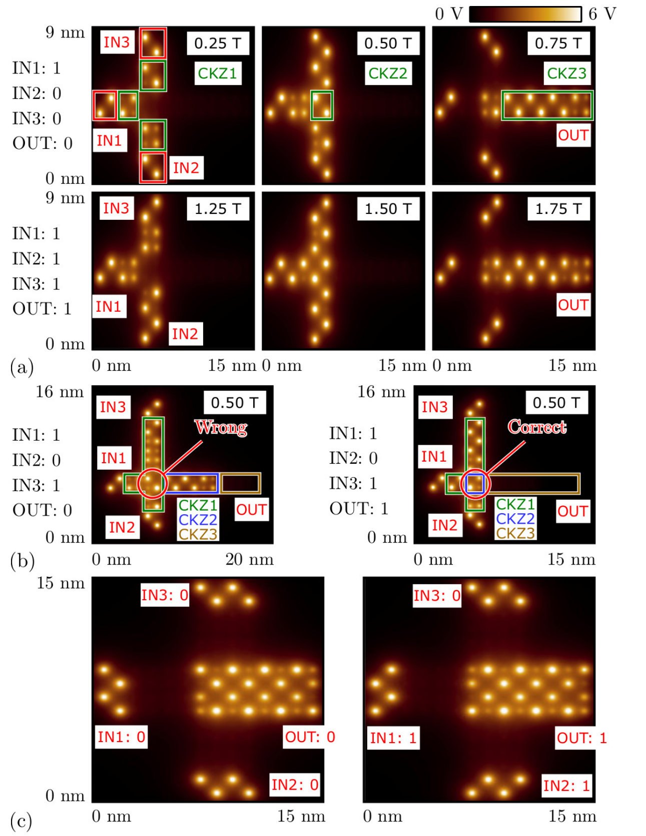

Fig. 8. SCERPA simulation of a clocked molecular FCN majority voters partitioned into three clock zones (CKZ1, CKZ2, CKZ3). The figure reports the electrostatic potential generated by the molecule charge distribution evaluated 0.2 nm above the active dot plane. (a) simple molecular majority voter. (b) molecular majority voter with input wires different in the number of cells; if the evaluation point and the input wires are in the same clock zone (left) an error occurs. An independent central clock zone (right) allows preventing errors. (c) 2-lines molecular majority voter.

physical verification of FCN circuits intended to confirm high-level simulation results based on the general QCA paradigm, encouraging the designer to seek eventual alternative layouts. Considering the promising results obtained for the other devices, we focus on the clocked 2-lines molecular inverter, shown in Fig. 2(b). Fig. 9(c) shows the SCERPA simulation. Initially, the logical value ‘0’ propagates in the first clock zone ($t = 0.25T$) and is copied ($t = 0.5T$) by the two lateral branches of the device. At $t = 0.75T$, the third clock zone is activated. The interaction at the interface between CK2 and CK3 produces the inversion of the logical information, thus logical output is ‘1’.

At $t = 1.00T$, the logical input is changed to ‘1’. As a consequence of the pipelining mechanism, the logical output remains ‘1’. After the application of a second clock cycle, the inverter output becomes ‘1’ at $t = 1.75T$.

F. The molecular XOR

The inverter and the majority voter permit the realization of any logic function. As an example, we design a XOR logic gate by combining the previously shown 2-lines devices.

Fig. 10(a) shows the complete layout occupying an area approximately equal to 0.002 μm^2. We partition each device

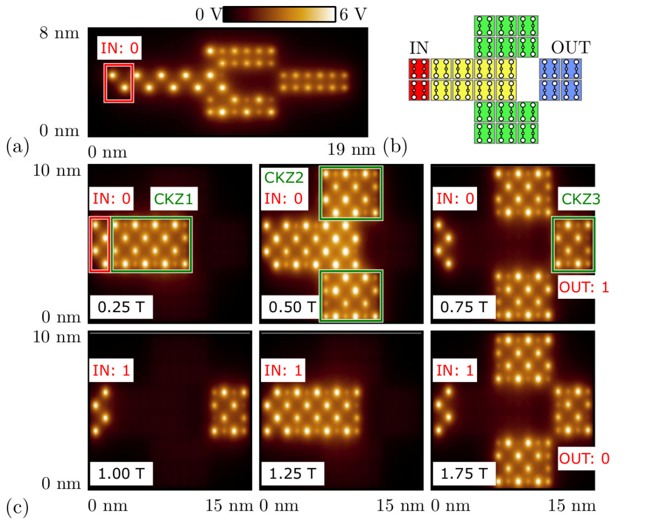

Fig. 9. (a) SCERPA simulation of a standard clocked molecular FCN inverter, layout is reported in Fig. 2. The figure reports the electrostatic potential generated by molecule charge distribution evaluated 0.2 nm above the active dot plane. (b) Layout of a 2-lines clocked molecular FCN inverter partitioned into three clock zones. (c) SCERPA simulation of the 2-lines clocked molecular FCN inverter.

into four clock zones. Assuming T be the clock cycle period. Each clock zone introduces a $T/4$ delay, whereas logic gates (i.e. 4 clock zones) introduce a T delay. Between inputs (named A and B) and output (Y), there are three pipelining stages: the total delay of the device is $3T$ (latency is 3), yet the XOR input can be changed every period T (i.e. the throughput is $1/T$). Fig. 10(b) displays the logical information propagating in the device with respect to the time. SCERPA computed 135 steps, with physical precision, in 114 min (single-core computation on Intel(R)Core(TM) i7-8565U 1.80 GHz). We focus, as a chance, on $t = 3T$, Fig. 10(c) shows a snapshot of the entire circuit at this precise time.

Time $3T$ coincides with the circuit delay. Indeed, the logical output is '0': the result of the XOR operation of the with "0-0" input configuration of time $t = 0$. At the output of the two majority gates ($\bar{A}B$ and $A\bar{B}$), the logical values '1' and '0' associated with the configuration "1-0" of time $t = 2T$ show up. These two values will be processed in the following clock cycle by the final majority voter, giving as result '1'. At the same time, the two input inverters $\bar{A}$ and $\bar{B}$ invert the input configuration "1-0" of time $t = 2T$ whereas the current input is "1-1", supposed to be ready at time $t = 6T$.

This result proves the SCERPA functionality on more sophisticated devices. For the first time, we demonstrate with physical simulation the possibility to exploit the clock mechanism to guide the information propagation among several simple molecular FCN devices, assembled to create more complex logic functions. This novel result paves the way for the future design of complex circuits by assessing SCERPA as a possible algorithm for CAD tool simulation engine.

V. Conclusion

The molecular Field-Coupled Nanocomputing (FCN) has been recommended as one of the most exciting technology for future digital electronics. The SCERPA algorithm has been used in previous works to analyze molecular circuits, modeling the molecule as an electronic device, and keeping the link between the logic behavior of the circuit and the physical aspects of the technology.

In this work, we extend SCERPA to the simulation of clocked devices. We provide a methodology to consider the clock field in the algorithm, and we demonstrate that SCERPA efficiently simulates molecular circuits with a multi-phase clock system, demonstrating their correct logic behavior in a pipeline structure. We demonstrate that molecular devices made with 2-lines structures make the information encoding stability stronger, as well as reducing the required technological resolution and facilitating the realization of an eventual prototype. Concerning the majority voter, we demonstrate, with physical simulation, that precise control of the central cell improves the device robustness. Finally, we show the physical simulation of a possible XOR, with a well-designed clocking layout. The obtained results confirm the possibility of implementing the QCA paradigm at the molecular scale. This work highlights that molecular physics poses a requirement for the simulation tool. Indeed, proper corrections must be made for the molecular device to work, and these corrections must be verified with physical simulations. High-level simulators can be used to study device functional behavior, yet physical simulation is mandatory to validate the obtained design.

In conclusion, we extended SCERPA to evaluate the performance of clocked molecular FCN devices. The algorithm provides essential feedback to circuit designers and technologists, paving the way for the future design of complex circuits via CAD tools, and further motivating research in this field to eventually facilitate the realization of a molecular prototype.

References

[1] A. O. Orlov, I. Amlani, G. H. Bernstein, C. S. Lent, and G. L. Snider, "Realization of a functional cell for quantum-dot cellular automata," *Science*, vol. 277, no. 5328, pp. 928–930, 1997.

[2] A. Orlov, A. Imre, G. Csaba, L. Ji, W. Porod, and G. H. Bernstein, "Magnetic quantum-dot cellular automata: Recent developments and prospects," *Journal of Nanoelectronics and Optoelectronics*, vol. 3, no. 1, pp. 55–68, 2008.

[3] C. S. Lent, B. Isaksen, and M. Lieberman, "Molecular quantum-dot cellular automata," *Journal of the American Chemical Society*, vol. 125, no. 4, pp. 1056–1063, 2003. PMID: 12537505.

[4] Y. Lu, M. Liu, and C. Lent, "Molecular quantum-dot cellular automata: From molecular structure to circuit dynamics," *Journal of Applied Physics*, vol. 102, no. 3, p. 034311, 2007.

[5] M. T. Niemier, *The effects of a New Technology on the Design, Organization, and Architectures of Computing System*. PhD thesis, University of Notre Dame, Notre Dame, IN, USA, 1993.

[6] C. S. Lent, P. D. Tougaw, W. Porod, and G. H. Bernstein, "Quantum cellular automata," *Nanotechnology*, vol. 4, no. 1, p. 49, 1993.

[7] L. Zoli, *Active bis-ferrocene molecules as unit for molecular computation*. PhD thesis, Università di Bologna, Bologna, Italy, 2010.

[8] V. Arima, M. Iurlo, L. Zoli, S. Kumar, M. Piacenza, F. Della Sala, F. Matino, G. Maruccio, R. Rinaldi, F. Paolucci, M. Marcaccio, P. G. Cozzi, and A. P. Bramanti, "Toward quantum-dot cellular automata units: thiolated-carbazole linked bisferrocenes," *Nanoscale*, vol. 4, no. 3, pp. 813–823, 2012.

[9] V. Vankamamidi, M. Ottavi, and F. Lombardi, "Clocking and cell placement for qca," in *2006 Sixth IEEE Conference on Nanotechnology*, vol. 1, pp. 343–346, July 2006.

[10] R. Wang, A. Pulimeno, M. R. Roch, G. Turvani, G. Piccinini, and M. Graziano, "Effect of a clock system on bis-ferrocene molecular qca," *IEEE Transactions on Nanotechnology*, vol. 15, pp. 574–582, July 2016.

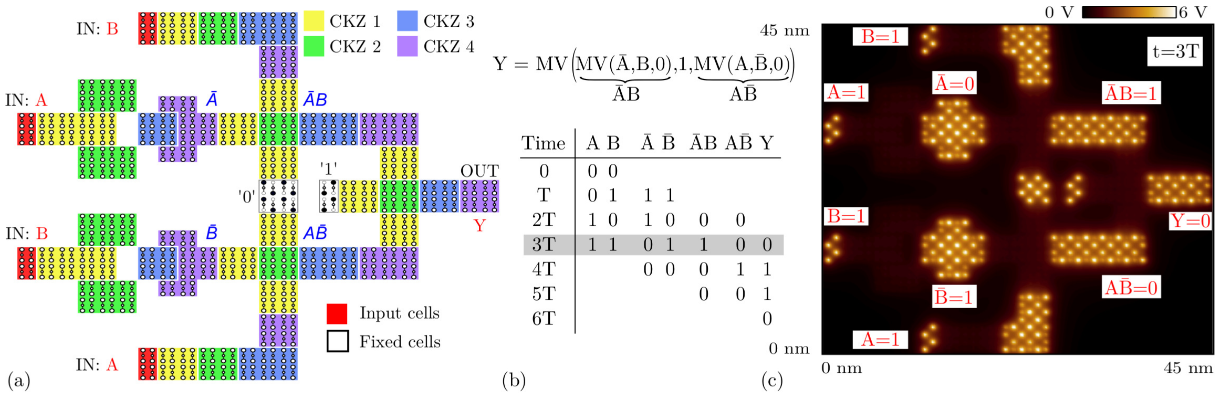

Fig. 10. (a) Layout of a clocked molecular FCN XOR partitioned into four clock zones (CKZ1, CKZ2, CKZ3, CKZ4). (b) XOR pipeline mechanism. (c) SCERPA simulation of the XOR: electrostatic potential generated by the molecule charge distribution evaluated 0.2 nm above the active dot plane.

[11] G. Tóth and C. S. Lent, "Quasiadiabatic switching for metal-island quantum-dot cellular automata," *Journal of Applied Physics*, vol. 85, no. 5, pp. 2977–2984, 1999.

[12] V. Vankamamidi, M. Ottavi, and F. Lombardi, "Two-dimensional schemes for clocking/timing of qca circuits," *IEEE Transactions on Computer-Aided Design of Integrated Circuits and Systems*, vol. 27, pp. 34–44, Jan 2008.

[13] F. Riente, U. Garlando, G. Turvani, M. Vacca, M. Ruo Roch, and M. Graziano, "Magcad: Tool for the design of 3-d magnetic circuits," *IEEE Journal on Exploratory Solid-State Computational Devices and Circuits*, vol. 3, pp. 65–73, Dec 2017.

[14] K. Walus, T. J. Dysart, G. A. Jullien, and R. A. Budiman, "Qcadesigner: a rapid design and simulation tool for quantum-dot cellular automata," *IEEE Transactions on Nanotechnology*, vol. 3, pp. 26–31, March 2004.

[15] Y. Ardesi, R. Wang, G. Turvani, G. Piccinini, and M. Graziano, "Scerpa: A self-consistent algorithm for the evaluation of the information propagation in molecular field-coupled nanocomputing," *IEEE Transactions on Computer-Aided Design of Integrated Circuits and Systems*, vol. 39, no. 10, pp. 2749–2760, 2020.

[16] M. Vacca, G. Turvani, F. Riente, M. Graziano, D. Demarchi, and G. Piccinini, "Tamtams: An open tool to understand nanoelectronics," in *Nanotechnology (IEEE-NANO), 2012 12th IEEE Conference on*, pp. 1–5, Aug 2012.

[17] R. Wang, M. Chilla, A. Palucci, M. Graziano, and G. Piccinini, "An effective algorithm for clocked field-coupled nanocomputing paradigm," in *2016 IEEE Nanotechnology Materials and Devices Conference (NMDC)*, pp. 1–2, Oct 2016.

[18] M. Graziano, R. Wang, M. R. Roch, Y. Ardesi, F. Riente, and G. Piccinini, "Characterisation of a bis-ferrocene molecular qca wire on a non-ideal gold surface," *Micro Nano Letters*, vol. 14, no. 1, pp. 22–27, 2019.

[19] Y. Ardesi, L. Gnoli, M. Graziano, and G. Piccinini, "Bistable propagation of monostable molecules in molecular field-coupled nanocomputing," in *2019 15th Conference on Ph.D Research in Microelectronics and Electronics (PRIME)*, pp. 225–228, July 2019.

[20] A. Pulimeno, M. Graziano, D. Demarchi, and G. Piccinini, "Towards a molecular qca wire: simulation of write-in and read-out systems," *Solid-State Electronics*, vol. 77, pp. 101 – 107, 2012. Special Issue of IEEE INEC 2011(IEEE International Nano Electronics Conference).

[21] Yuliang Wang and M. Lieberman, "Thermodynamic behavior of molecular-scale quantum-dot cellular automata (qca) wires and logic devices," *IEEE Transactions on Nanotechnology*, vol. 3, pp. 368–376, Sep. 2004.

[22] C. S. Lent and B. Isaksen, "Clocked molecular quantum-dot cellular automata," *IEEE Transactions on Electron Devices*, vol. 50, pp. 1890–1896, Sep. 2003.

[23] Y. Ardesi, A. Pulimeno, M. Graziano, F. Riente, and G. Piccinini, "Effectiveness of molecules for quantum cellular automata as computing devices," *Journal of Low Power Electronics and Applications*, vol. 8, no. 3, 2018.

[24] P. D. Tougaw and C. S. Lent, "Logical devices implemented using quantum cellular automata," *Journal of Applied Physics*, vol. 75, no. 3, pp. 1818–1825, 1994.

[25] M. Awais, M. Vacca, M. Graziano, and G. Masera, "Fft implementation using qca," in *2012 19th IEEE International Conference on Electronics, Circuits, and Systems (ICECS 2012)*, pp. 741–744, Dec 2012.

[26] M. Awais, M. Vacca, M. Graziano, M. R. Roch, and G. Masera, "Quantum dot cellular automata check node implementation for ldpc decoders," *IEEE Transactions on Nanotechnology*, vol. 12, pp. 368–377, May 2013.

[27] J. A. Christie, R. P. Forrest, S. A. Corcelli, N. A. Wasio, R. C. Quardokus, R. Brown, S. A. Kandel, Y. Lu, C. S. Lent, and K. W. Henderson, "Synthesis of a neutral mixed-valence diferrocenyl carborane for molecular quantum-dot cellular automata applications," *Angewandte Chemie International Edition*, vol. 54, no. 51, pp. 15448–15451, 2015.

[28] L. Verstraete, P. Szabelski, A. M. Bragança, B. E. Hirsch, and S. De Feyter, "Adaptive self-assembly in 2d nanoconfined spaces: Dealing with geometric frustration," *Chemistry of Materials*, vol. 31, no. 17, pp. 6779–6786, 2019.

[29] J. N. Randall, J. W. Lyding, S. Schmucker, J. R. Von Ehr, J. Ballard, R. Saini, H. Xu, and Y. Ding, "Atomic precision lithography on si," *Journal of Vacuum Science & Technology B: Microelectronics and Nanometer Structures Processing, Measurement, and Phenomena*, vol. 27, no. 6, pp. 2764–2768, 2009.

[30] L.-J. Wang, G. Cao, T. Tu, H.-O. Li, C. Zhou, X.-J. Hao, Z. Su, G.-C. Guo, H.-W. Jiang, and G.-P. Guo, "A graphene quantum dot with a single electron transistor as an integrated charge sensor," *Applied Physics Letters*, vol. 97, no. 26, p. 262113, 2010.

[31] F. Mohn, L. Gross, N. Moll, and G. Meyer, "Imaging the charge distribution within a single molecule," *Nature nanotechnology*, vol. 7, pp. 227–31, 02 2012.

[32] A. Pulimeno, M. Graziano, A. Sanginario, V. Cauda, D. Demarchi, and G. Piccinini, "Bis-ferrocene molecular qca wire: Ab initio simulations of fabrication driven fault tolerance," *IEEE Transactions on Nanotechnology*, vol. 12, pp. 498–507, July 2013.

[33] D. Tougaw, "A clocking strategy for scalable and fault-tolerant qdca signal distribution in combinational and sequential devices," in *Field-Coupled Nanocomputing*, 2014.

[34] C. S. Lent and G. L. Snider, *The Development of Quantum-Dot Cellular Automata*, pp. 3–20. Berlin, Heidelberg: Springer Berlin Heidelberg, 2014.

[35] A. Pulimeno, M. Graziano, R. Wang, D. Demarchi, and G. Piccinini, "Charge distribution in a molecular qca wire based on bis-ferrocene molecules," in *2013 IEEE/ACM International Symposium on Nanoscale Architectures (NANOARCH)*, pp. 42–43, July 2013.

[36] E. San-Fabián Maroto and J.-C. Sancho-García, "Emerging dft methods and their importance for challenging molecular systems with orbital degeneracy," *Computation*, vol. 7, no. 4, 2019.

[37] A. Pulimeno, M. Graziano, A. Antidormi, R. Wang, A. Zahir, and G. Piccinini, *Understanding a Bisferrocene Molecular QCA Wire*, pp. 307–338. Berlin, Heidelberg: Springer Berlin Heidelberg, 2014.

[38] M.J. Frisch et al, "Gaussian09 revision a.1," 2009. Gaussian Inc.Wallingford CT.

[39] K. Hennessy and C. S. Lent, "Clocking of molecular quantum-dot cellular automata," *Journal of Vacuum Science & Technology B: Microelectronics and Nanometer Structures Processing, Measurement, and Phenomena*, vol. 19, no. 5, pp. 1752–1755, 2001.

[40] Y. Mahmoodi and M. A. Tehrani, "Novel fault tolerant qca circuits," in *2014 22nd Iranian Conference on Electrical Engineering (ICEE)*, pp. 959–964, 2014.